Ce³⁺ 4f¹ Pr³⁺ 4f² Nd³⁺ 4f³ Pm³⁺ 4f⁴ Sm³⁺ 4f⁵ Eu³⁺ 4f⁶ Gd³⁺ 4f⁷

Tb³⁺ 4f⁸ Dy³⁺ 4f⁹ Ho³⁺ 4f¹⁰ Er³⁺ 4f¹¹ Tm³⁺ 4f¹² Yb³⁺ 4f¹³ Lu³⁺ 4f¹⁴

INORGANIC
CHEMISTRY
FRONTIERS

RESEARCH ARTICLE

Stable iso-bacteriochlorin mimics from porpholactone: effect of a β-oxazolone moiety on the frontier π-molecular orbitals†

Yi Yu,[a] Taniyuki Furuyama,[b] Juan Tang,[a] Zhuo-Yan Wu,[a] Jia-Zhen Chen,[a] Nagao Kobayashi*[b] and Jun-Long Zhang*[a]

Iso-bacteriochlorins known as siroheme in some reductases, featured with two adjacent reduced pyrrole rings, have distinctive electronic structures from porphyrin, chlorin and bacteriochlorin analogues. However, the synthesis of such cofactor mimics from hydrogenation of chlorin or porphyrin is associated with drawbacks of uncertain regioselectivity and stability. In this work, we present the first example of selective hydrogenation of the adjacent pyrroles in porphyrin or porpholactone free bases assisted by the Woollins reagent (WR). More importantly, adjacent-dihydroporpholactone (**1a**) displays iso-bacteriochlorin type spectral features and much higher stability under oxidative conditions, compared to the tetrahydro-porphyrin analogue (**2a**). Analysis of magnetic circular dichroism (MCD) spectra and DFT calculations for the frontier π-molecular orbitals for **1a** and **2a** reveals the significant effect of a β-oxazolone moiety replacement on lowering the HOMO energy level and enhancing the stability resistant to oxidative conditions.

Introduction

Tetrapyrroles are distributed as biological cofactors with diverse biochemical roles such as light absorption characteristics, redox catalytic reactivity, *etc*.[1] Significant diversity in biological functions suggests the importance of electronic differences, arising from the saturation levels of tetrapyrrole rings with their broad structural similarity.[2] To decipher the chemical basis, the development of synthetic hydroporphyrins to mimic the electronic structures of natural tetrapyrroles becomes one of the key areas in current synthetic porphyrin chemistry.[3] An iso-bacteriochlorin, featured with two adjacent reduced pyrrole rings, plays an important role in sulfite and nitrite reductases as a prosthetic group[4] (known as siroheme, Scheme 1) and as a key intermediate in the biosynthetic pathway to vitamin B12.[5] However, synthesis of such mimics is challenging and fraught with a number of problems such as (1) stability, suffering from an easy oxidation back to a porphyrin (or other products); and (2) uncertain regioselectivity,

[a]Beijing National Laboratory for Molecular Sciences, State Key Laboratory of Rare Earth Materials Chemistry and Applications, College of Chemistry and Molecular Engineering, Peking University, Beijing 100871, P.R. China.
E-mail: zhangjunlong@pku.edu.cn; Fax: +86-10-62767034
[b]Department of Chemistry, Graduate School of Science, Tohoku University, Sendai 980-8578, Japan. E-mail: nagaok@m.tohoku.ac.jp
†Electronic supplementary information (ESI) available. CCDC 1047515. For ESI and crystallographic data in CIF or other electronic format see DOI: 10.1039/c5qi00054h

Scheme 1 Structural formulae of siroheme, porphyrin and porpholactone and hydrogenated analogues.

lack of methodology to selective hydrogenation of adjacent pyrroles from chlorin or porphyrin free bases. Although total synthesis or semi-synthesis by the joining of eastern and western dipyrrolic components have been reported,[6] multiple synthetic steps with small scales thus diminish the practical value. Thus, a new approach to stable iso-bacteriochlorin mimics is highly desirable to expand the scope of hydroporphyrins,[2a,7] in a manner that should facilitate the fundamental understanding of the electronic structures and further applications.

As our continued interest in porpholactone,[8] in which one pyrrole of porphyrin is replaced by an oxazolone (or lactone) moiety (Scheme 1), we envisioned that this replacement might facilitate to stabilize the hydroporphyrins by lowering the HOMO energy level. Moreover, for the partial saturated oxazolone replacement, selective hydrogenation of the adjacent pyrroles of the oxazolone moiety might achieve iso-bacteriochlorin mimics. This would circumvent the regioselectivity issue by tuning the electronic effect of substituents on the porphyrin periphery, according to a theoretical study by Bruhn and Brückner.[9] In this work, we report the first example of selective hydrogenation of the adjacent pyrroles in porphyrin or porpholactone free bases assisted by the Woollins reagent $(PhPSe_2)_2$. More importantly, adjacent-dihydroporpholactone (**1a**) displays iso-bacteriochlorin like spectral features and much higher stability under oxidative conditions, compared to tetrahydroporphyrin analogue (**2a**). To decipher the effect of β-oxazolone on the electronic structures, we performed magnetic circular dichroism (MCD) spectroscopy and DFT calculations to analyze the relative energies of the frontier π-molecular orbitals and hence on the optical properties. These results suggested that the higher stability of **1a** is due to the decreased HOMO energy level after replacing the β-oxazolone moiety. Furthermore, we applied **1a** as a cell imaging agent by encapsulating into poly(lactide-co-glycolide) nanoparticles and demonstrated its good stability and luminescence. Thus, this work provides an access to stable iso-bacteriochlorin like analogue and highlights the importance of β-oxazolone moiety replacement on further studying natural tetrapyrrole mimics.

Results and discussion

To evaluate the effect of the β-oxazolone moiety on the stability of hydroporphyrins, we firstly estimated the molecular structures and molecular orbital (MO) diagrams of adjacent-dihydro-porpholactones (**1a**) and tetrahydroporphyrin analogue (**2a**) derivatized from tetrapentafluorophenylporpholactone ($H_2F_{20}TPPL$, **1**) and tetrapentafluorophenylporphyrin ($H_2F_{20}TPP$, **2**), at the B3LYP/6-31G* level using the Gaussian 09 package, on the basis of Gourterman's four orbital model. As shown in Fig. 1, for **1a** and **2a**, the hydrogenation of tetrapyrrole rings leads to less degenerate MOs, which is in accordance with those for previously reported iso-bacteriochlorin analogues.[2c] For the β-oxazolone moiety that participated in the π-conjugation, the energies of four frontier orbitals of **1a** are evidently lowered than those of **2a**, especially for HOMO and LUMO levels (ca. 0.46 and 0.50 eV, respectively). Thus, on the basis of DFT calculations, the replacement of the β-oxazolone moiety renders iso-bacteriochlorin mimics **1a** more resistant to oxidative conditions.

Synthesis of iso-bacteriochlorin mimics 1a and 2a

Regioselectivity is another important issue yet to be addressed in the synthesis of iso-bacteriochlorin mimics. Generally, the
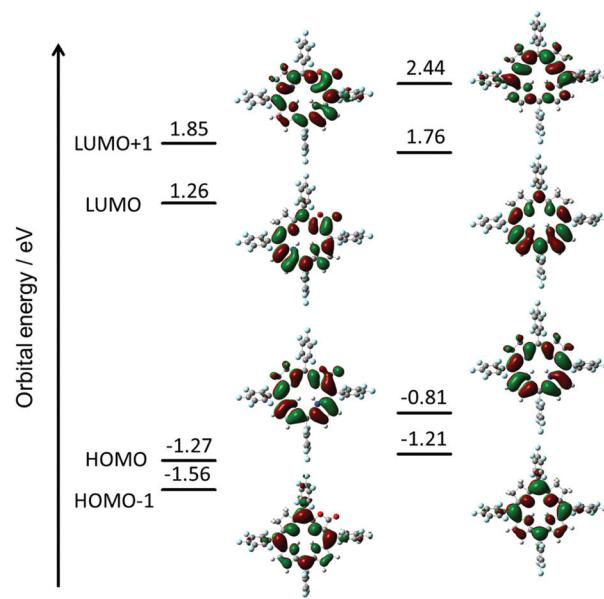
Fig. 1 Molecular orbital diagrams of **1a** (left) and **2a** (right), optimized at the B3LYP/6-31 G* level using the Gaussian 09 software package.

reactions of diimide based reductants,[7j,10] or electrophilic agents such as OsO_4,[8h,11] ozone[12] or dienes[13] or 1,3-dipoles such as azomethine ylides, nitrones, or nitrile oxides,[14] with chlorin or porphyrin free bases afforded bacteriochlorin type hydroporphyrin (the opposite pyrroles were hydrogenated), while with metallochlorin or porphyrin lead to metalloisobacteriochlorins. In this work, attempts to hydrogenation of **1** to **1a** using previous methods such as photoreduction[7i] or reducing with diimide[7j] failed. We then turned our attention to the selenium-assisted reduction system based on Woollins' reagent (WR).[15] Since Jaisankar et al. demonstrated the effectiveness in hydrogenation of aromatic ketones,[16] WR based reduction procedures had been extended to selective hydrogenation of the C=C bond in α,β-unsaturated carbonyl compounds, though the mechanisms were still unclear.[17] As shown in Scheme 2, the reaction of 1 eq. WR, **1** and 4 eq. $PhMe_2SiH$ in refluxed toluene gave the adjacent-dihydroporpholactone **1a** in an isolated yield of 40%. We did not observe the product that Se replaces an O atom of the carbonyl group. ESI-MS showed a molecular ion peak at m/z = 995.0543 (ca. 995.0557), consistent with the dihydrogenation of one pyrrole in **1a**. The ^1H NMR spectrum ($CDCl_3$) displayed three sets of peaks at 7.28, 7.54 and 7.74 ppm (β-H, 4H), two sets of multiple peaks at 3.86 and 3.82 ppm (C–H at reduced pyrrole, 4H) and two broad protons at 3.97 and 4.86 ppm (N–H, 2H) which would disappear after coordination with the Zn^{2+} ion (ESI†). The splitting of ^{19}F signals at −138, −153 and −162 ppm illustrated lower symmetry than that of porpholactone **1**. The vibration of C=O at 1780 cm^{-1} on the IR spectrum showed that the lactone moiety remained intact (1766 cm^{-1} for **1**). The UV-vis spectrum of **1a** (will discuss in the next section) displays iso-bacteriochlorin type absorption.
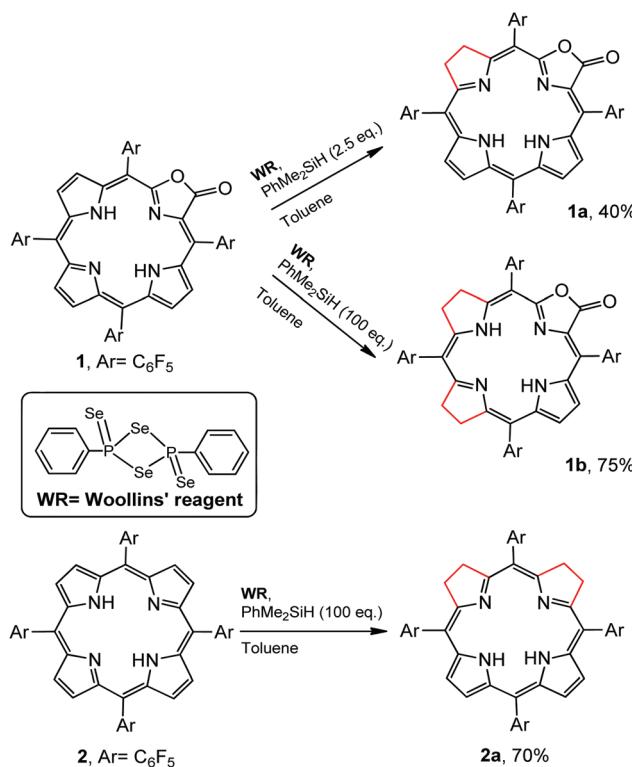
Scheme 2 Synthetic routes for **1a**, **1b** and **2a**.

Fig. 2 (a) ORTEP diagram of **Zn1a** (thermal ellipsoids at the 30% probability level); (b) selected bond distances (Å) for the core of **Zn1a**; (c) edge-on-views of the core of **Zn1a** along the N2–N3–N4 planes.

Similarly, tetrahydroporphyrin **2a** was obtained using **2** as a precursor in the isolated yield of 70% (ESI†). A large excess amount of silane (100 equiv.) in the synthesis of **2a** was used, probably due to two adjacent pyrroles that required to be hydrogenated other than one pyrrole in **1a**. To confirm this, we increased the amount of silane to 100 equiv. in the reaction of **1** with WR, and found that tetrahydroporpholactone **1b** was obtained in the yield of 75% (characterization in the ESI†). **1b** and **2a** also exhibit iso-bacteriochlorin type spectra as previously reported tetraphenylporphyrin analogues.[2a,18] It is worthy to note that, in the absence of WR or PhMe$_2$SiH, the formation of **1a**, **1b** or **2a** was not observed. Interestingly, no reaction was observed using metalloporpholactone **Zn1** or metalloporphyrin **Zn2** as a starting material under the same conditions. Metalation of **1a**, **1b** and **2a** with Zn(OAc)$_2$ in methanol produced **Zn1a**, **Zn1b** and **Zn2a** (the details listed in the ESI†). These results demonstrated that the protocol containing WR and silane is effective to directly reduce the adjacent double bond of porpholactone and porphyrin free bases.

To clarify where hydrogenation takes place, we tried to grow the single crystals of **1a** however, we could not get the plausible data due to the disorder of the lactone moiety. Metalation of **1a** with the Zn^{2+} ion produced **Zn1a** and the single crystal suitable for X-ray diffraction could be obtained in the presence of pyridine (CCDC: 1047515). In Fig. 2, the ORTEP structure shows that the additional hydrogens are located on the pyrrole adjacent to the oxazolone ring (oxa-atom side). It is reflected by the elongated C6–C7 bond length (1.473 Å) relative to the

other pyrroles (C11–C12 and C16–C17: 1.365 and 1.407 Å), which is comparable to 1.479 and 1.497 Å in previously reported adjacent-(tetrahydrotetraphenylporphinato)(pyridine) zinc(II).[19] Similar 1.481 Å and 1.498 Å are also observed in C5–C6 and C7–C8 bond distances (1.472 Å to 1.508 Å in the case of (adjacent-tetrahydrotetraphenylporphinato)(pyridine) zinc(II)). The Zn–N2 distance is 2.122 (5) Å, which is longer than the other three Zn–N distances (2.023 (4) Å, 2.075 (4) Å and 2.100 (5) Å). The torsion angle of C$_\alpha$C$_\beta$C$_\beta$C$_\alpha$ of the reduced pyrrole ring is 4.23°, indicating the twist (0.86° and 2.40° for the other two conjugated pyrrole rings) in the porphyrin ring.

Photophysical properties

To better demonstrate the effect of the replacement of the β-oxazolone moiety, we discuss the photophysical properties of **1a** and **2a** in the context. The electronic absorption of **1a**, **2a** and their zinc complexes in CH$_2$Cl$_2$, as shown in Fig. 3(a), display iso-bacteriochlorin type spectra with broader, split, and blue-shifted Soret bands.[2d,4f,18a] Compared with **1** and **2**, **1a** and **2a** also exhibit broad, intense and blue-shifted Q bands at 500–610 nm, indicating the degeneracy of molecular orbitals and slightly increasing HOMO–LUMO gaps due to lower molecular symmetry after hydrogenation. For **1a**, there is small absorption with maxima at 636 nm, which disappears after metallation with the Zn^{2+} ion (Fig. 3(a)). Thus, this absorption is assumed to be a partial protonation of pyrroles, further verified by using the acid titration experiment as shown in Fig S7.† However, for **2a**, the absorption at *ca.* 750 nm does not disappear even in **Zn2a**, which might be due to the contamination of trace bacteriochlorin for less selective reduction of porphyrin **2**. Compared with the free bases, Zn complexes show red shifts of the absorption bands. In particular, the difference of Q(0,0) bands between **1a** and **Zn1a** is 43 nm, which is larger than that between **2a** and **Zn2a** (14 nm), respectively. The red shifts of absorption bands indicate less macrocycle distortion of Zn complexes and enhancing π-conjugation.

This journal is © the Partner Organisations 2015

Inorg. Chem. Front., 2015, **2**, 671–677 | **673**
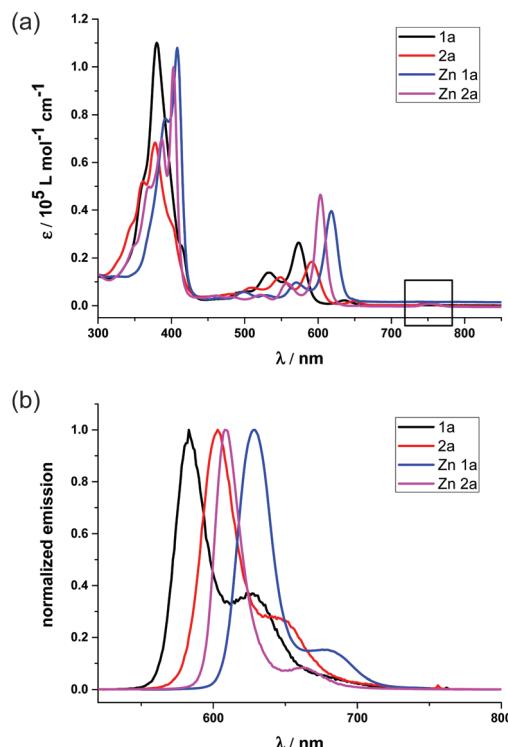
Fig. 3 (a) Absorption spectra of **1a** (black), **2a** (red), **Zn1a** (blue) and **Zn2a** (purple) in CH_2Cl_2; (b) normalized emission spectra of **1a** (black), **2a** (red), **Zn1a** (blue) and **Zn2a** (purple) in CH_2Cl_2. Concentrations are all 5.0×10^{-6} M, and all excited at maximum absorption.

The fluorescence spectra of **1a** and **2a** in Fig. 3(b) display peak maxima (λ_{max}) at 583 nm and 603 nm with a shoulder at 625 and 654 nm, respectively. The fluorescence quantum yields and fluorescence lifetimes were determined to be 0.47 and 3.88 ns for **1a**, 0.55 and 5.63 ns for **2a**, respectively. After metallization, the quantum yield and lifetime of **Zn1a** were 0.13 and 0.70 ns, while 0.08 and 1.08 ns for **Zn2a**. Thus, radiative and non-radiative decay rates were calculated to be $k_r = 1.2 \times 10^8$ and $k_{nr} = 1.4 \times 10^8$ s^{-1} for **1a**, $k_r = 9.8 \times 10^7$ and $k_{nr} = 9.8 \times 10^7$ s^{-1} for **2a**, $k_r = 1.9 \times 10^8$ and $k_{nr} = 1.2 \times 10^9$ s^{-1} for **Zn1a**, $k_r = 7.4 \times 10^7$ and $k_{nr} = 8.5 \times 10^8$ s^{-1} for **Zn2a**, respectively.

The electrochemical properties were studied by cyclic voltammetry in CH_2Cl_2 (*vs.* ferrocene 0.45 V as a standard, Table S2, Fig. S13 and S14†). Compared with **1** and **2**, **1a** and **2a** display cathodic shifts of *ca.* 0.37 and 0.61 V, respectively, for the first oxidation potentials; and *ca.* 0.21–0.33 V for the first reduction potentials. The first oxidation potential of **1a** (1.33 V) is more positive than **2a** (0.92 V) whereas there is a lesser difference in the first reduction potentials between **1a** (−0.78 V) and **2a** (−1.13 V). A similar trend was observed for **Zn1a** and **Zn2a**, in which the first oxidation potential of **Zn1a** (0.99 V) is 0.37 V higher than that of **Zn2a** (0.62 V). Again, these electrochemical studies clearly showed that the replacement of the β-oxazolone moiety lowers the first oxidative potentials of hydroporphyrins more than the first reduction potentials, given that similar HOMO–LUMO gaps are obtained

from UV-vis absorption for **1a** and **2a**, **Zn1a** and **Zn2a**. This is consistent with the trend of energies of four frontier orbitals and HOMO–LUMO gaps for **1a** and **2a** based on DFT calculations.

Stability

Stabilities of **1a**, **2a**, **Zn1a** and **Zn2a** were examined under oxidative conditions using *m*-CPBA, DDQ and light irradiation (ESI†). We used UV-vis absorption and ^{1}H NMR spectroscopy to monitor the reaction process. **1a** and **Zn1a** exhibited high stability and remained intact when treated with 10 eq. *m*-CPBA for 1 day or irradiated with light at 365 nm for 2 h. **2a** decomposed upon addition of *m*-CPBA in 2 h or light irradiation for 90 min (88%, calculated based on ^{1}H NMR integration). **Zn2a** was very unstable toward oxidation or UV irradiation, and even decomposition was observed on the silica gel column. These results clearly demonstrated that the oxazolone replacement indeed stabilized the reduced porphyrinoid structures, in line with electrochemical and theoretical studies.

MCD spectroscopy and DFT calculation

To further demonstrate the advantage of porpholactone, we used **1a**, **Zn1a**, **2a** and **Zn2a** to discuss the effect of oxazolone replacement on the photophysical properties and electronic structures. The electronic absorption and MCD spectra of these complexes in CH_2Cl_2 are shown in Fig. 4. Compared with normal porphyrins which have four unsaturated pyrrole rings, the intensity of the Q band is much stronger, so that the Q/Soret intensity ratio is stronger than in normal porphyrins. According to the Gouterman's four orbital theory that has been applied in understanding spectra of porphyrinoids,[20] this indicates that the energy difference between the HOMO and HOMO−1 (ΔHOMO) is larger than that in normal porphyrins. Due to the uncertainty of the position of two pyrrole protons and the presence of several isomers, the spectra of metal-free **1a** and **2a** are more complex than those of the **Zn1a** and **Zn2a**. For **1a**, there is a small absorption with a maximum at 636 nm. This absorption is ascribed to the partial protonation of pyrroles, which is verified by using the acid titration experiment, and which disappears after metallation with the Zn^{2+} ion. The Zn complexes show red-shifted absorption compared with those of metal-free species. In particular, the difference of the Q$_{00}$ bands between **1a** and **Zn1a** is 43 nm, which is larger than that between **2a** and **Zn2a** (14 nm). The spectra of **1a** and **Zn1a** are broadly similar to those of iso-bacteriochlorin whose two pyrrole rings at adjacent positions are reduced.[18a,21] The splitting of the Q band is theoretically not large, different from that of bacteriochlorin which has saturated pyrrole rings at opposite positions.[22]

For complexes in this study, the MCD spectra are all contribution of Faraday B terms.[23] The observed spectra were interpreted in consideration of the results of MO calculations. Although the MCD spectra are complex for metal-free species, the most decisive difference between **1a** and **2a** is that the MCD sign for the Q$_{00}$ band is positive for **1a** and negative for **2a** in ascending energy, experimentally suggesting that the

674 | *Inorg. Chem. Front.*, 2015, **2**, 671–677

This journal is © the Partner Organisations 2015
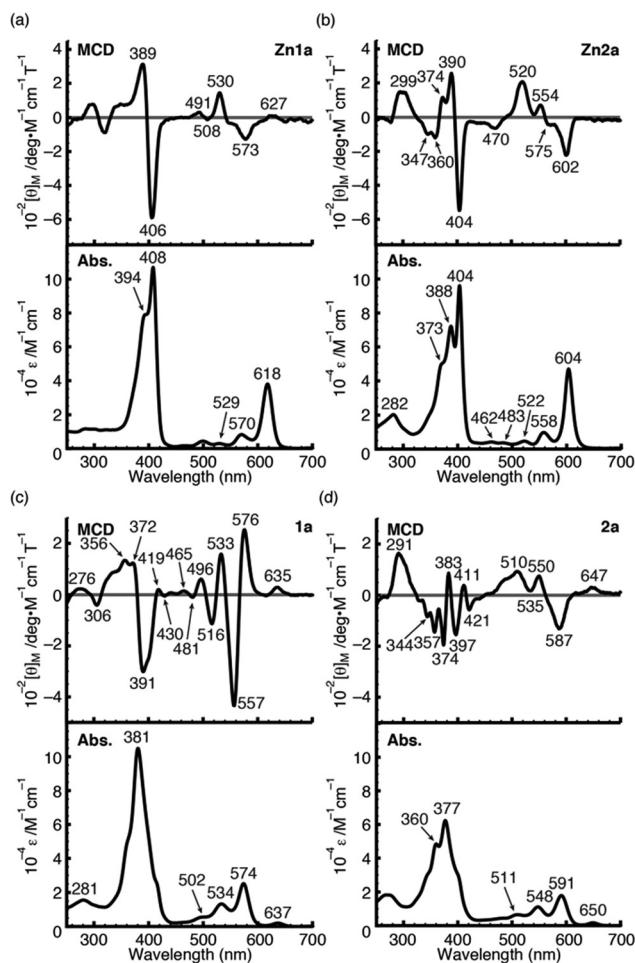
Fig. 4 MCD (top) and UV/Vis (bottom) absorption spectra of **Zn1a** (a), **Zn2a** (b), **1a** (c) and **2a** (d) in CH$_2$Cl$_2$.

Fig. 5 Calculated frontier orbitals of **Zn1a** (left) and **Zn2a** (right).

ΔHOMO is smaller than ΔLUMO (the energy difference between the LUMO and LUMO+1) for **1a** and opposite for **2a**.[23] The MCD spectra of **Zn1a** and **Zn2a** appear similar at a glance, but there is a decisive difference in the Q band region, namely, for **Zn2a**, a clear negative MCD envelope was observed corresponding to the Q$_{00}$ absorption peak at 604 nm, indicating that ΔHOMO is obviously larger than ΔLUMO.[23] Meanwhile for **Zn1a**, no (or very small positive) MCD intensity was observed associated with the Q$_{00}$ band at 616 nm, indicating experimentally that ΔHOMO is nearly equal to ΔLUMO. Judging from the MCD sign, another important information is that the peak at 570 nm for **Zn1a** and 558 nm for **Zn2a** correspond to the split components of the Q band, since the interacting MCD B-terms give signals of an opposite sign.[23,24] Taking all the MCD data of **1a**, **2a**, **Zn1a**, and **Zn2a** into account, it is experimentally concluded that ΔHOMO is much larger than ΔLUMO for **2a** and **Zn2a**, while that the ΔHOMO is similar to or very slightly smaller than ΔLUMO for **1a** and **Zn1a**. We have calculated molecular orbitals (MOs) of **Zn1a** and **Zn2a**, hence we don't need to consider the position of pyrrole protons that occurred for metal-free **1a** and **2a**. The data are shown in

Fig. 5. Compared with the MOs of **Zn2a**, those of **Zn1a** are all from the calculation, and the above relationship on the size of ΔHOMO and ΔLUMO was nicely reproduced, *i.e.* they are 0.61 and 0.60 eV for **Zn1a** and 0.79 and 0.32 eV for **Zn2a**, respectively.

Fluorescence and cell imaging

Since β-lactonization of the pyrrole ring renders hydroporphyrins higher stability, we used **1a** as an example to demonstrate their potential application in cellular imaging. To make it water-soluble, we used the modified solvent extraction/evaporation single-emulsion method to prepare **1a**-loaded poly (lactide-*co*-glycolide) nanoparticles (PLGA NPs) as reported.[25] The intracellular luminescence and subcellular distribution of **1a-NPs** were investigated using the LysoTracker® Green DND-26 by confocal laser scanning microscopy (CLSM). HeLa cells were co-incubated with **1a-NPs** with a final concentration of 10 μM in complete culture medium for 24 h at 37 °C. As shown in Fig. 6, **1a-NPs** possess good cell membrane permeability and leads to the perinuclear punctate red fluorescence in HeLa cells. It mainly distributes in lysosomal/endosomal compartments and exhibits a co-localization level

This journal is © the Partner Organisations 2015

Inorg. Chem. Front., 2015, **2**, 671–677 | **675**
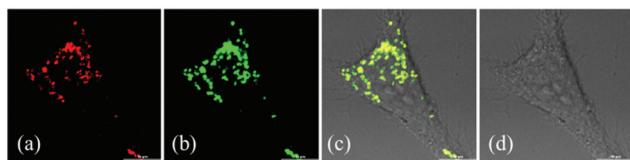
Fig. 6 Co-localization of **1a**-NPs (10 μM) with the LysoTracker® Green DND-26 in HeLa cells. (a) Fluorescence image of **1a**-NPs; (b) fluorescence image of the LysoTracker® Green DND-26; (c) the merge of (a), (b) and (d); (d) differential interference contrast (DIC) image. Scale bar: 10 μm.

of approximately 0.92 with the LysoTracker® Green DND-26. Thus, preliminary imaging results show **1a**-NPs can be internalized into living cells and detected by confocal imaging, which offers the prerequisite and convenience for further biological applications.

Conclusions

Taken together, we developed a new approach based on the Woollins reagent to prepare iso-bacteriochlorin mimics from porpholactone or porphyrin free bases. More importantly, with an oxazolone moiety replacement, β-adjacent dihydroporpholactone (**1a**) exhibits high stability toward oxidative conditions and photo-irradiation. A detailed analysis of optical spectra and TD-DFT calculations reveal that **1a** and **2a** possess electronic structures similar to iso-bacteriochlorins and the significant effect of the oxazolone moiety on lowering the HOMO energy level. Furthermore, cellular uptake and subcellular localization investigations have demonstrated the potential utility of these compounds in the biological studies. The application of such iso-bacteriochlorin analogues as ligands to mimic the reactivity of sulfite and nitrite reductases is currently under investigation.

Acknowledgements

Notes and references

1 (a) T. D. Lash, in *The Porphyrin Handbook*, ed. K. M. Kadish, K. M. Smith and R. Guilard, Academic Press, New York, 2000, vol. 2, pp. 125–200; (b) J. Mack, M. J. Stillman and N. Kobayashi, *Coord. Chem. Rev.*, 2007, **251**, 429–453; (c) J. L. Sessler, A. Gebauer and S. J. Weghorn, in *The Porphyrin Handbook*, ed. K. M. Kadish, K. M. Smith and R. Guilard, Academic Press, New York, 2000, vol. 2, pp. 55–124; (d) H. J. Xu, J. Mack,

A. B. Descalzo, Z. Shen, N. Kobayashi, X. Z. You and K. Rurack, *Chem. – Eur. J.*, 2011, **17**, 8965–8983.

2 (a) J. A. Cavaleiro, M. G. Neves, A. C. Tome, A. Silva, M. A. Faustino, P. S. Lacerda and A. M. Silva, *J. Heterocycl. Chem.*, 2000, **37**, 527–534; (b) A. Ghosh, *J. Phys. Chem. B*, 1997, **101**, 3290–3297; (c) N. Otero, S. Fias, S. Radenković, P. Bultinck, A. M. Graña and M. Mandado, *Chem. – Eur. J.*, 2011, **17**, 3274–3286; (d) P. Pershukevich, I. Shushkevich, E. Makarova and K. Solov'eva, *J. Appl. Spectrosc.*, 2008, **75**, 706–713.

3 (a) A. R. Battersby, *Nat. Prod. Rep.*, 2000, **17**, 507–526; (b) F.-P. Montforts, B. Gerlach and F. Hoeper, *Chem. Rev.*, 1994, **94**, 327–347.

4 (a) B. A. Averill, *Chem. Rev.*, 1996, **96**, 2951–2964; (b) B. R. Crane, L. M. Siegel and E. D. Getzoff, *Science*, 1995, **270**, 59–67; (c) R. J. Krueger and L. M. Siegel, *Biochemistry*, 1982, **21**, 2892–2904; (d) J. Liu, S. Chakraborty, P. Hosseinzadeh, Y. Yu, S. Tian, I. Petrik, A. Bhagi and Y. Lu, *Chem. Rev.*, 2014, **114**, 4366–4469; (e) L. B. Maia and J. J. Moura, *Chem. Rev.*, 2014, **114**, 5273–5357; (f) M. J. Murphy, L. M. Siegel, S. R. Tove and H. Kamin, *Proc. Natl. Acad. Sci. U. S. A.*, 1974, **71**, 612–616; (g) J. Vega and H. Kamin, *J. Biol. Chem.*, 1977, **252**, 896–909; (h) L. M. Siegel, M. J. Murphy and H. Kamin, *J. Biol. Chem.*, 1973, **248**, 251–264.

5 (a) A. Eschenmoser, *Angew. Chem., Int. Ed. Engl.*, 1988, **27**, 5–39; (b) J.-H. Martens, H. Barg, M. Warren and D. Jahn, *Appl. Microbiol. Biotechnol.*, 2002, **58**, 275–285; (c) E. Raux, C. Thermes, P. Heathcote, A. Rambach and M. J. Warren, *J. Bacteriol.*, 1997, **179**, 3202–3212; (d) A. I. Scott, *Angew. Chem., Int. Ed. Engl.*, 1993, **32**, 1223–1243; (e) A. I. Scott, A. J. Irwin, L. M. Siegel and J. Shoolery, *J. Am. Chem. Soc.*, 1978, **100**, 7987–7994.

6 (a) A. Battersby, P. Harrison and C. Fookes, *J. Chem. Soc., Chem. Commun*, 1981, **15**, 797–799; (b) A. R. Battersby, K. Frobel, F. Hammerschmidt and C. Jones, *J. Chem. Soc., Chem. Commun.*, 1982, 455–457; (c) M. H. Block, S. C. Zimmerman, G. B. Henderson, S. P. Turner, S. W. Westwood, F. J. Leeper and A. R. Battersby, *J. Chem. Soc., Chem. Commun.*, 1985, 1061–1063; (d) F. P. Montforts, S. Ofner, V. Rasetti, A. Eschenmoser, W. D. Woggon, K. Jones and A. R. Battersby, *Angew. Chem., Int. Ed. Engl.*, 1979, **18**, 675–677; (e) P. Naab, R. Lattmann, C. Angst and A. Eschenmoser, *Angew. Chem., Int. Ed. Engl.*, 1980, **19**, 143–145.

7 (a) J. M. de Souza, F. F. de Assis, C. Carvalho, J. A. Cavaleiro, T. J. Brocksom and K. T. de Oliveira, *Tetrahedron Lett.*, 2014, **55**, 1491–1495; (b) M. C. de Souza, L. F. Pedrosa, G. S. Cazagrande, V. F. Ferreira, M. G. Neves and J. A. Cavaleiro, *Beilstein J. Org. Chem.*, 2014, **10**, 628–633; (c) A. M. Silva, A. C. Tomé, M. G. Neves, A. M. Silva and J. A. Cavaleiro, *Chem. Commun.*, 1999, 1767–1768; (d) A. C. Tome, P. S. Lacerda, M. Neves and J. A. Cavaleiro, *Chem. Commun.*, 1997, 1199–1200; (e) A. Aggarwal, S. Thompson, S. Singh, B. Newton, A. Moore, R. Gao, X. Gu, S. Mukherjee and C. M. Drain, *Photochem. Photo-*

biol., 2014, **90**, 419–430; (*f*) S. Singh, A. Aggarwal, S. Thompson, J. P. Tomé, X. Zhu, D. Samaroo, M. Vinodu, R. Gao and C. M. Drain, *Bioconjugate Chem.*, 2010, **21**, 2136–2146; (*g*) Y. Harel and J. Manassen, *J. Am. Chem. Soc.*, 1978, **100**, 6228–6234; (*h*) D. J. Simpson and K. M. Smith, *J. Am. Chem. Soc.*, 1988, **110**, 2854–2861; (*i*) H. Tamiaki, M. Xu and T. Mizoguchi, *Tetrahedron Lett.*, 2012, **53**, 3210–3212; (*j*) H. W. Whitlock Jr., R. Hanauer, M. Oester and B. Bower, *J. Am. Chem. Soc.*, 1969, **91**, 7485–7489.

8 (*a*) Y. Yu, H. Lv, X. Ke, B. Yang and J. L. Zhang, *Adv. Synth. Catal.*, 2012, **354**, 3509–3516; (*b*) M. J. Crossley and L. G. King, *J. Chem. Soc., Chem. Commun.*, 1984, 920–922; (*c*) J. R. McCarthy, H. A. Jenkins and C. Bruckner, *Org. Lett.*, 2003, **5**, 19–22; (*d*) J. Akhigbe, C. Ryppa, M. Zeller and C. Brückner, *J. Org. Chem.*, 2009, **74**, 4927–4933; (*e*) L. Liang, H. B. Lv, Y. Yu, P. Wang and J. L. Zhang, *Dalton Trans.*, 2012, **41**, 1457–1460; (*f*) H. B. Lv, B. Y. Yang, J. Jing, Y. Yu, J. Zhang and J. L. Zhang, *Dalton Trans.*, 2012, **41**, 3116–3118; (*g*) M. Gouterman, R. J. Hall, G. E. Khalil, P. C. Martin, E. G. Shankland and R. L. Cerny, *J. Am. Chem. Soc.*, 1989, **111**, 3702–3707; (*h*) C. Bruckner, S. J. Rettig and D. Dolphin, *J. Org. Chem.*, 1998, **63**, 2094–2098.

9 T. Bruhn and C. Brückner, *J. Org. Chem.*, 2015, **80**, 4861–4868.

10 (*a*) J. M. Dabrowski, L. G. Arnaut, M. M. Pereira, C. J. P. Monteiro, K. Urbanska, S. Simoes and G. Stochel, *ChemMedChem*, 2010, **5**, 1770–1780; (*b*) M. M. Pereira, C. J. P. Monteiro, A. V. C. Simoes, S. M. A. Pinto, A. R. Abreu, G. F. F. Sa, E. F. F. Silva, L. B. Rocha, J. M. Dabrowski, S. J. Formosinho, S. Simoes and L. G. Arnaut, *Tetrahedron*, 2010, **66**, 9545–9551; (*c*) M. Pineiro, A. Gonsalves, M. M. Pereira, S. J. Formosinho and L. G. Arnaut, *J. Phys. Chem. A*, 2002, **106**, 3787–3795.

11 (*a*) C. Bruckner and D. Dolphin, *Tetrahedron Lett.*, 1995, **36**, 9425–9428; (*b*) H. Fischer and H. Eckoldt, *Justus Liebigs Ann. Chem.*, 1940, **544**, 138–162; (*c*) C. K. Chang, C. Sotiriou and W. Wu, *J. Chem. Soc., Chem. Commun.*, 1986, 1213–1215; (*d*) Y. H. Chen, C. J. Medforth, K. M. Smith, J. Alderfer, T. J. Dougherty and R. K. Pandey, *J. Org. Chem.*, 2001, **66**, 3930–3939; (*e*) J. M. Sutton, N. Fernandez and R. W. Boyle, *J. Porphyrins Phthalocyanines*, 2000, **4**, 655–658.

12 A. M. Shulga, I. M. Biteva, I. F. Gurinovich, L. A. Grubina and G. P. Gurinovich, *Biofizika*, 1977, **22**, 771–776.

13 (*a*) A. C. Tome, P. S. S. Lacerda, A. M. G. Silva, M. Neves and J. A. S. Cavaleiro, *J. Porphyrins Phthalocyanines*, 2000, **4**, 532–537; (*b*) A. C. Tome, P. S. S. Lacerda, M. Neves and J. A. S. Cavaleiro, *Chem. Commun.*, 1997, **13**, 1199–1200.

14 (*a*) M. C. de Souza, L. F. Pedrosa, G. S. Cazagrande, V. F. Ferreira, M. Neves and J. A. S. Cavaleiro, *Beilstein J. Org. Chem.*, 2014, **10**, 628–633; (*b*) J. M. de Souza, F. F. de

Assis, C. M. B. Carvalho, J. A. S. Cavaleiro, T. J. Brocksom and K. T. de Oliveira, *Tetrahedron Lett.*, 2014, **55**, 1491–1495; (*c*) A. Aggarwal, S. Thompson, S. Singh, B. Newton, A. Moore, R. M. Gao, X. B. Gu, S. Mukherjee and C. M. Drain, *Photochem. Photobiol.*, 2014, **90**, 419–430; (*d*) A. M. G. Silva, A. C. Tome, M. Neves, A. M. S. Silva and J. A. S. Cavaleiro, *Chem. Commun.*, 1999, 1767–1768; (*e*) A. M. G. Silva, A. C. Tome, M. Neves, A. M. S. Silva, J. A. S. Cavaleiro, D. Perrone and A. Dondoni, *Tetrahedron Lett.*, 2002, **43**, 603–605.

15 (*a*) J. C. Fitzmaurice, D. J. Williams, P. T. Wood and J. D. Woollins, *J. Chem. Soc., Chem. Commun.*, 1988, 741–743; (*b*) I. P. Gray, P. Bhattacharyya, A. M. Slawin and J. D. Woollins, *Chem. – Eur. J.*, 2005, **11**, 6221–6227; (*c*) M. J. Pilkington, A. M. Slawin, D. J. Williams, P. T. Wood and J. D. Woollins, *Heteroat. Chem.*, 1990, **1**, 351–355; (*d*) P. T. Wood and J. D. Woollins, *J. Chem. Soc., Chem. Commun.*, 1988, 1190–1191.

16 M. Mandal, S. Chatterjee and P. Jaisankar, *Synlett*, 2012, 2615–2618.

17 (*a*) Y. Nishiyama, J. Inoue, K. Teranishi, M. Moriwaki and S. Hamanaka, *Tetrahedron Lett.*, 1992, **33**, 6347–6350; (*b*) Y. Nishiyama, Y. Makino, S. Hamanaka, A. Ogawa and N. Sonoda, *Bull. Chem. Soc. Jpn.*, 1989, **62**, 1682–1684.

18 (*a*) H. Miwa, E. A. Makarova, K. Ishii, E. A. Luk'yanets and N. Kobayashi, *Chem. – Eur. J.*, 2002, **8**, 1082–1090; (*b*) A. B. J. Parusel and A. Ghosh, *J. Phys. Chem. A*, 2000, **104**, 2504–2507.

19 K. M. Barkigia, J. Fajer, L. D. Spaulding and G. J. B. Williams, *J. Am. Chem. Soc.*, 1981, **103**, 176–181.

20 M. Gouterman, *J. Mol. Spectrosc.*, 1961, **6**, 138–163.

21 N. Kobayashi, H. Miwa and V. N. Nemykin, *J. Am. Chem. Soc.*, 2002, **124**, 8007–8020.

22 (*a*) C. J. Ballhausen, *Introduction to Ligand field Theory*, McGraw-Hill, New York, 1962; (*b*) H. Konami and N. Kobayashi, in *The Phthalocyanines-Properties and Applications*, ed. A. B. P. L. C. C. Leznoff, VCH, Weinheim, 1996, vol. 4, ch. 9.

23 (*a*) J. Michl, *J. Am. Chem. Soc.*, 1978, **100**, 6801–6811; (*b*) J. Michl, *J. Am. Chem. Soc.*, 1978, **100**, 6812–6818; (*c*) J. Michl, *Pure Appl. Chem.*, 1980, **52**, 1549–1563; (*d*) J. M. N. Kobayashi, *Circular Dichroism and Magnetic Circular Dichroism Spectroscopy for Organic Chemists*, Royal Society of Chemistry, London, 2011.

24 A. Tajiri and J. Winkler, *Z. Naturforsch., A: Phys. Sci.*, 1983, **38**, 1263–1269.

25 (*a*) K. Li, J. Pan, S. S. Feng, A. W. Wu, K. Y. Pu, Y. Liu and B. Liu, *Adv. Funct. Mater.*, 2009, **19**, 3535–3542; (*b*) Z. Zhang, S. Tongchusak, Y. Mizukami, Y. J. Kang, T. Ioji, M. Touma, B. Reinhold, D. B. Keskin, E. L. Reinherz and T. Sasada, *Biomaterials*, 2011, **32**, 3666–3678.

This journal is © the Partner Organisations 2015

Inorg. Chem. Front., 2015, **2**, 671–677 | **677**